Determination of the Deflection of a Cantilever Beam and Poisson's Ratio by Holographic Interferometry

Dr. Jumlong Limtragool*

[Received for publication April 5, 1989]

Abstract

This paper discusses about the technique to determine the surface deflection of a cantilever beam subjected to a point load by using a double-exposure holographic interferometry. The computer generated holographic fringe pattern compares very well with the experimental result. The obtained fringe pattern represents both deflection and anticlastic behavior of the surface of the beam due to the three dimensional effect. Combining the anticlastic behavior with the beam theory we could get poisson's ratio of the material. Experimental result using aluminium alloy 6061-T6 as a cantilever beam indicates that its poisson's ratio is equal to 0.355 which agrees with the value in the published data to within 2.3%

---

* Associate Professor, Mechanical Engineering Department, Faculty of Engineering, Khon Kaen University, Khon Kaen 40002.

การหาค่าระยะยุบตัวและอัตราส่วนพัวซองของคานยื่น โดยใช้ภาพการสอดแทรกแบบสามมิติ

ดร. จำลอง ลิ้มตระกูล*

บทคัดย่อ

บทความนี้กล่าวถึงวิธีการหาค่าระยะยุบตัวที่ผิวของคานยื่นเมื่ออยู่ภายใต้แรงกระทำแบบจุด โดยใช้ภาพการสอดแทรกแบบสามมิติ ชนิดฉายซ้ำสองครั้ง ภาพการสอดแทรกแบบสามมิติ ที่สร้างขึ้นโดยคอมพิวเตอร์มีลักษณะเหมือนกันกับผลที่ได้จากการทดลอง เส้นการสอดแทรกแสดงถึงลักษณะการยุบตัวและการแอ่นตัวแบบอานม้าที่ผิวของคาน ซึ่งเป็นผลมาจากลักษณะสามมิติของชิ้นงาน เมื่อรวม ลักษณะการแอ่นตัวเข้ากับทฤษฎีของคาน เราสามารถหาค่าอัตราส่วนพัวซองของวัสดุได้ ผลจากการทดลอง โดยใช้อลูมิเนียมผสมเบอร์ 6061-T6 ทำคาน พบว่าอัตราส่วนพัวซองมีค่าเท่ากับ 0.355 ซึ่งผิดพลาดไปจากค่าที่มีอยู่ในเอกสารที่พิมพ์เผยแพร่เพียง 2.3 %

1. Introduction

The wavefront reconstruction technique or holography is an optical method which allows one to record and reproduce a three

---

* รองศาสตราจารย์ ประจำภาควิชาวิศวกรรมเครื่องกล คณะวิศวกรรมศาสตร์ มหาวิทยาลัยขอนแก่น 40002

dimensional image of an object. In 1948, D. Gabor [1] discovered that if a coherent wave is made to interfere with the diffracted wave from an object, then the whole information, i.e., both amplitude and phase of the object wave can be recorded. From such a recorded interference pattern called hologram, an image of the original object can be seen during the reconstruction process even though the object has been removed.

In holographic interferometry (HI) two states of the object from the recorded hologram are compared interferometrically during the reconstruction process. An interference fringe pattern, due to the differential change of the surface displacement fields between the two states, will form and superimpose on the virtual or real image of the specimen. The fringe pattern acts as a gaging element for measuring changes in the surface displacements of the specimen. Applications of HI for measuring displacement components were made by several investigators [2-7].

In this paper, HI technique was used to measure the deflection of a cantilever beam subjected to a point load. The fringe pattern gives the surface deflection contour of the beam and also the anticlastic behavior of the beam. Combining the later with the beam theory, poisson's ratio of the beam material was found.

2. Holographic Interferometry

In HI, the three-dimensional image of an objcet from the two different states, which have been recorded in the hologram are compared interferometrically during the reconstruction process. With this technique, deformation, displacement or rotation of the object

can be recorded holographically in terms of the interference fringe patterns. They are basically three types of HI, i.e,

a) Double-exposure HI,

b) Real-time HI, and

c) Time-average HI.

2.1 Double-exposure HI In this method the first exposure is made when the object is in an undeformed or reference state and the second exposure is made on the same photographic plate when the object is in a deformed state. When the hologram is illuminated by the original reference beam one will see through it a three-dimensional virtual image of the object overlaid with an interference fringe pattern due to displacements between the two exposures. These fringes are called frozen fringes.

2.2 Real-Time HI The film plate is exposed only once in real-time HI, when the object is in the initial state. After developing, the hologram is then repositioned exactly in the same place so that the virtual image superimposes exactly on the object. When the object is deformed, live fringes will form in the virtual image. Thus, deformation of the object can be investigated in real-time through interference fringes.

2.3 Time-average HI In time-average HI, a vibrating object is hologrammed for analysis. Only a single exposure is required, but an exposure time has to be longer than the period of vibration. A series of images will be recorded since the object is vibrating during the exposure. For sinusoidal motion, the object will spend most of its time at the maximum vibrating excursions resulting in two primary images. During the reconstruction of the hologram, it will show

interference fringes due to these two images.

In double-exposure HI, the intensity distribution for both the virtual and real images through the hologram is given by

$$I = C(1+ \cos \Delta\varphi) \qquad .....1)$$

where C = constant due to amplitude of light intensity

$\Delta\varphi$ = change in optical phase due to deformation of the object

$(1 + \cos\Delta\varphi)$ = interference fringe pattern

3. Deflection of a Cantilever Beam

In terms of fringe order and optical path different, $\Delta\varphi$ can be written as

$$\Delta\varphi = 2\pi N$$

$$\Delta\varphi = (2\pi/\lambda)(\vec{k}_o - \vec{k}_i).\vec{d} \qquad .....2)$$

For measuring deflection of the cantilever beam, optical arrangement as shown in Fig. 1 was used. From Fig.1 the displacement Vector $\vec{d}$ and the propagation vectors $\vec{k}_1$ and $\vec{k}_o$ are given by:

$$\vec{d} = u\vec{i} + v\vec{j} + w\vec{k}$$

$$\vec{k}_i = -\sin\theta_i\vec{i} - \cos\theta_i\vec{k}$$

$$\vec{k}_o = -\sin\theta_o\vec{i} + \cos\theta_o\vec{k} \qquad .....3)$$

Substituting equation 3) into equation 2) and rearranging yields

$$(\sin\theta_i - \sin\theta_o)u + (\cos\theta_i + \cos\theta_o)w = N\lambda$$

and for $\theta_i = \theta_o$, one gets

$$w = N\lambda/(2\cos\theta_i) \qquad .....4)$$

where N = 0,1,2,.....for bright fringes

09234
24 มี.ค. 2533
มหาวิทยาลัยขอนแก่น

Equation 4) gives the deflection w of the beam in terms of fringe order N, wavelength of laser light and the incident angle θ_i

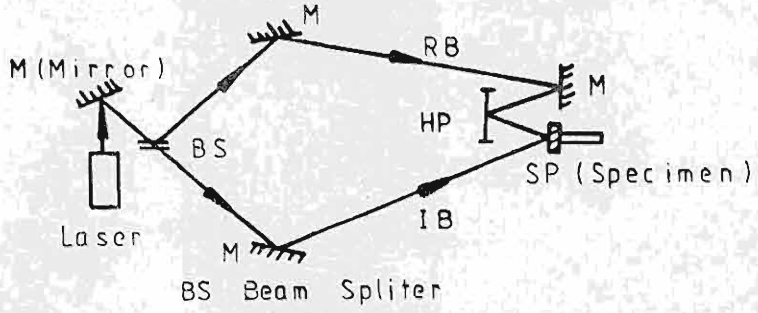

a) HI optical path arrangement

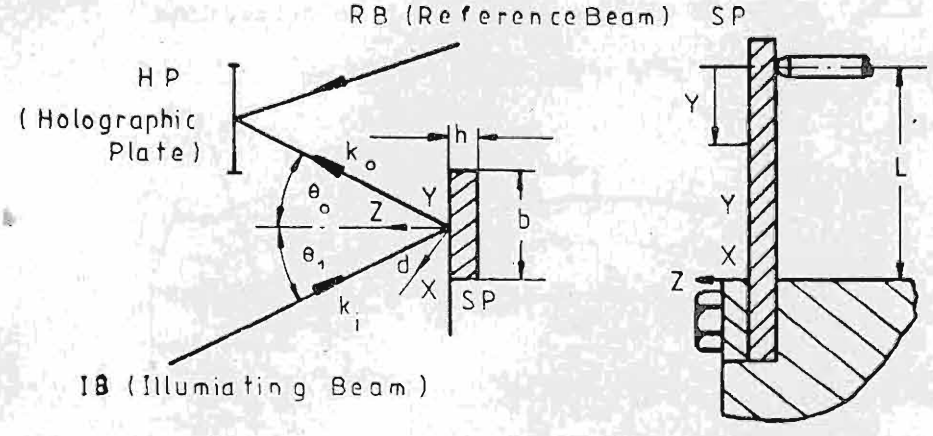

b) Geometry of the optical path for HI arrangement

Fig. 1 HI arrangement for deflection measurement

4. Poisson's Ratio Determination

Fig. 2 shows holographic fringe pattern due to deflection w = 25.4 μm at a distance L = 63.5 mm from fixed end of the cantilever beam. Near fixed end fringes bend upward. Equation 4) tells us that the surface deflection across the width of the beam at any section y varies symmetrically about the center of the width, This is the wellknown anticlastic behavior of the beam which is controlled by poisson's ratio of the material.

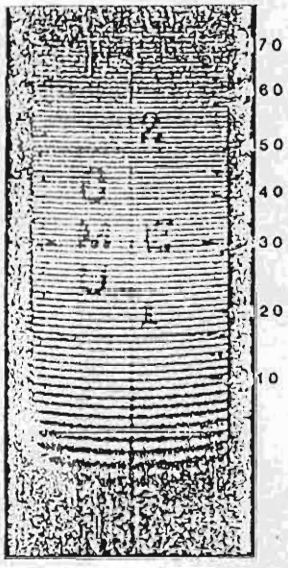

Fig.2 HI fringe pattern due to deflection

w = 25.4 μm at L = 63.5 mm

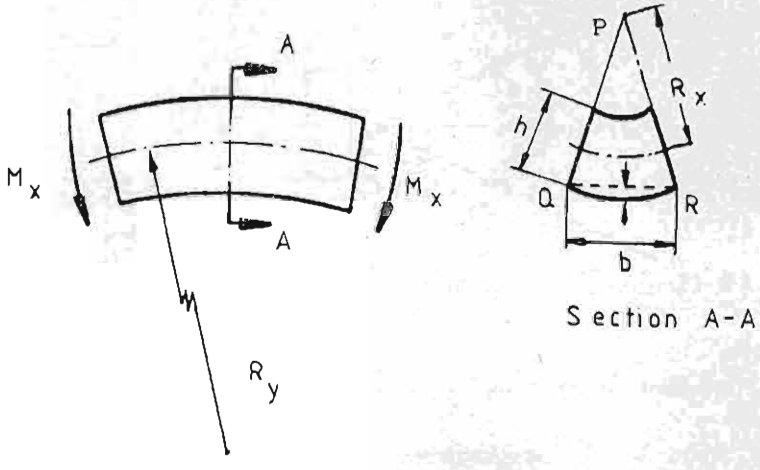

Fig.3 Pure bending of beam.

From beam theory, curvature of the beam in the x-and y-direction due to pure bending are given by (see Fig 3)

$$1/R_x = -\nu/R_y \text{ and } 1/R_y = M_x/(EI_x) \qquad \text{.....5)}$$

Assuming for the first approximation that Equation 5) is also valid for the case of a cantilever beam under load F as shown in Fig 4.

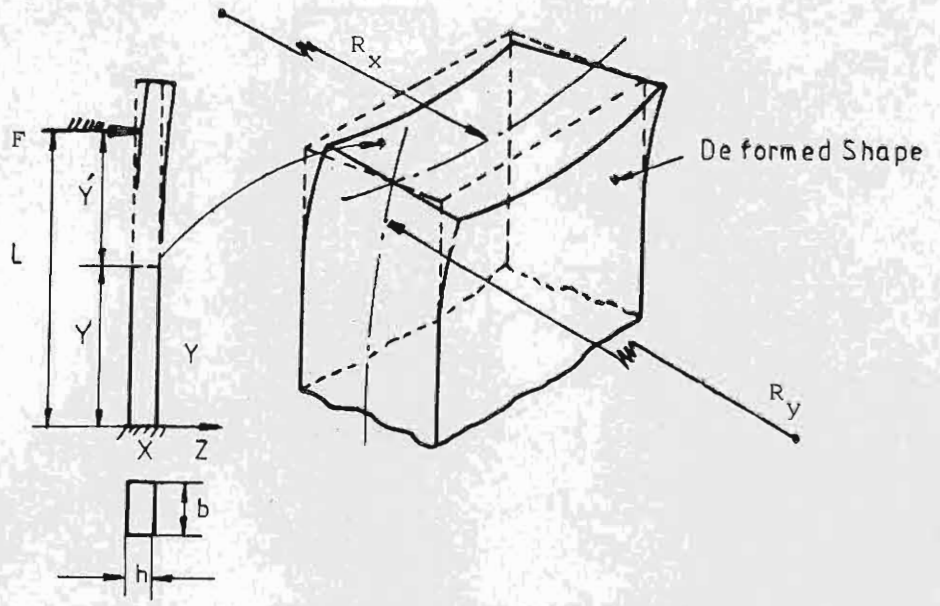

Fig. 4 Deformed shape of a cantilever beam subjected to a point load F.

Consider at any section y′ from F, the radius of curvature in the x-direction is related to the geometry of the beam as follows (see Fig.3):

$$(R_x + \tfrac{1}{2}h)^2 = (R_x + \tfrac{1}{2}h - \delta)^2 + (\tfrac{1}{2}b)^2 \qquad .....6)$$

Rearranging Equation 6) and assuming that $\frac{1}{2}b >> \delta$ and $R_x >> 1/2h$, then

$$R_x = (b^2/8\delta) \qquad .....7)$$

Substituting Equation 7) into Eqation 5) yields

$$\nu = 8(EI_x/Fb^2)[\delta(y)/y'] \qquad .....8)$$

where $M_x = Fy'$, and $\delta = \delta(y)$

$\delta(y)$ may be obtained from the fringe pattern. Consider at any section y' from load F (see Fig. 5), we get

$$\delta(y) = w_{cy} - w_{ey} \qquad .....a)$$

Substituting Equation 4) into Equation a),yields

$$\delta(y) = (\lambda/2 \cos \theta_i)(N_{cy} - N_{ey}) \qquad .....9)$$

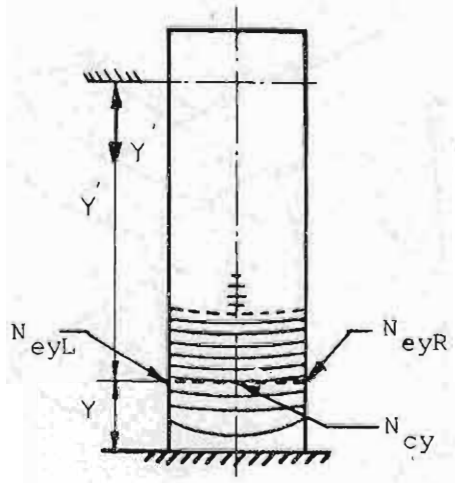

Fig. 5

Substituting Equation 9) into Equation 8), one gets poisson's ratio as follows:

$$\nu = 4(EI_x/F)(\lambda/b^2 \cos\theta_i)\,[(N_{cy} - N_{ey})/y'] \quad .....10)$$

From simple beam theory, deflection w at any section y from the fixed end of a cantilever beam due to load F is :

[for $o < y < L$] $w = (FL^3/6EI_x)[3(Y/L)^2 - (Y/L)^3]$ .....b)

[at $Y = L$] $\therefore w_L = FL^3/(3EI_x)$ .....c)

Substituting Equation (c) into Equation 10) yields

$$\nu = (4\lambda b/3w_L \cos\theta_i)(L/b)^3\,[(N_{cy} - N_{ey})/y'] \quad .....11)$$

Equation 11) gives the relationship between poisson's ratio and the known parameters from the geometry, loading and fringe pattern of the cantilever beam.

5. Computer Generated Holographic Fringe Pattern (CGHFP)

The three-dimensional finite element elastic code called SHAPES [8] was used to calculate the deflection of the cantilever beam subjected to a point load. The finite element model shown in Fig. 6

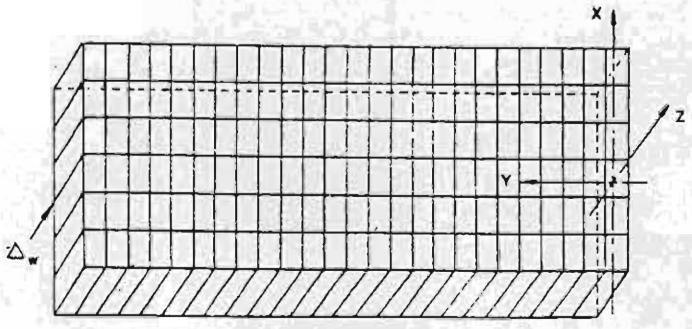

Fig.6 Finite element model of a cantilever beam

used only the linear strain isoparametric elements. It has 150 elements, 364 nodes and 1092 degree of freedoms. A deflection $w = 25.4\ \mu m$ was applied at a distance 63.5 mm from the fixed end. The beam is made of aluminium alloy 6061-T6. By using Equations 1), 2) and 4) and the surface deflection data from the finite element analysis, the computer generated holographic fringe pattern was generated as shown in Fig. 7. It agrees very well with the experimentally obtained fringe pattern as shown in Fig. 2 Details of the CGHFP technique can be found elsewhere [7].

6. Experimental Results

The cantilever beam used in this work is made of aluminium alloy 6061-T6. Fig. 2 shows the fringe pattern due to deflection $w = 25.4\ \mu m$ at a distance $L = 63.5$ mm from the fixed end. A He-Ne gas laser with a wavelength $\lambda = 6328\ \mathring{A}$ was used. The incident angle $\theta_i = 34$ degrees.

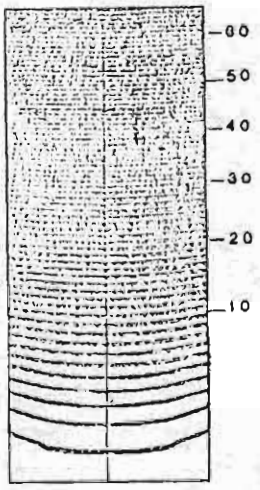

Fig.7 Computer generated holographic fringe pattern due to deflection of the cantilever beam subjected to a point load.

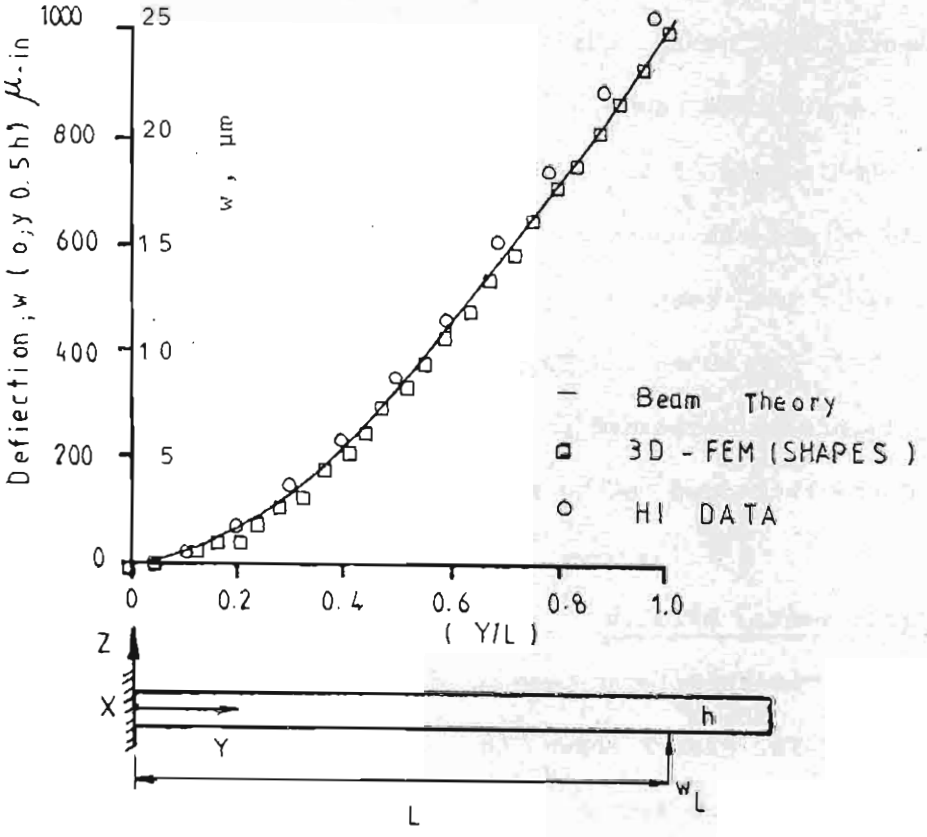

Fig. 8 Deflection of the beam

From Fig. 2 and Equation 4) graph of the beam deflection is shown in Fig. 8 together with the result from beam theory and the three-dimensional finite element analysis. The experimental result compared quite well with the results from beam theory and computer simulation.

For poisson's ratio, Equation 14) gives the prediction for left and right edge at any section y'from F. For example, considering at section y' = 38.1 mm, the fringe order at the center line and both edges are given as follows :

$$N_{cy} = 17.5, \quad N_{eyL} = 16.7, \quad \text{and} \quad N_{eyR} = 16.6$$

Substituting the relevant parameters into Equation 14) , we get

$$\nu = 15.9029[N_{cy} - N_{ey})/y']$$

for left edge, $\nu_L = 0.334$

for right edge, $\nu_R = 0.376$

and $\nu_{average} = \frac{1}{2}(\nu_R + \nu_L) = 0.355$

From the published data [9], $\nu = 0.347$ for aluminium alloy 6061-T6 which agrees quite well with the experimental result obtained from the technique in this work.

7. Conclusions

Deflection of a cantilever beam made of aluminium alloy 6061-T6 subjected to a point load was measured by using double-exposure HI. The deflection obtained from the experiment compared quite well with the results from beam theory and computer simulation. Due to poisson's ratio effect, the fringe pattern was

curved upward. This was because of the anticlastic behavior of the beam. Combining this effect with the beam theory, poisson's ratio of the material was found and agreed quite well with the published data. The computer generated holographic fringe pattern due to the deflection of the cantilever beam was generated from the data obtained from the three-dimensional finite element analysis. The computer generated fringe pattern compared very well with the experimentally obtained fringe pattern.

8. Notation

b width of the beam

C light from the image of an object, constant

$\vec{d}$ displacement vector

E Young's modulus

F point load

h thickness of the beam

I intensity distribution of the image

I_x second moment of area around x-axis

$\vec{i}$ unit vector in the x-direction

$\vec{j}$ unit vector in the y-direction

$\vec{k}$ unit vector in the z-direction

L length of the beam

M_x bending moment around x-axis

N fringe order

N_{cy} fringe order at the center of the beam at any section y

N_{ey} fringe order at the edge the beam at any section y

R_x, R_y radius of curvature in the x-and y-direction

u displacement in the x-direction

v displacement in the y-direction

w displacement in the z-direction

y distance along the length of the beam

δ the difference between the deffection of the center of the beam and its edge.

$\Delta\varphi$ optical phase difference

θ_i incident angle

θ_o reflection angle

λ wavelength of the light

ν poisson's ratio

BS beam splitter

HI holographic interferometry

HP holographic plate

IB illuminating beam

RB reference beam

9. Acknowledgement

The author wishes to express his sincere gratitude to Professr Dr. W.F. Stokey, Carnegie-Mellon University, PGH, PA, U.S.A., for his valuable comments and suggestions.

10. References

1. Gabor, D. (1948) , A New Microscopic, Nature, Vol 161, No. 4098, pp. 777-778.

2. Boone, P.M. and Verbiest (1969), Application of Holographic Interferometry to Plate Deformation and Translation Measurements,

Optica Acta, Vol. 16, No. 5 , pp. 555-567.

3. Ranson, W.R. (1971), Use of Holographic Interferometry to Determine the Surface Displacement of a Deformed Body, Tech. report, T&AM Report U. of Ill.

4. Hecht, N.L. (1972), Investigation of Holcgraphic Interferometry for Displacement Measurements, PH.D. Dissertation, Alfred Univ., USA. (May 1972),.

5. Gilbert, J.A. (1975), Optical Technique to Separate Compcnent of Displacements Using Holographic Interferometry, PH.D. Dissertation, Ill. Institute of Tech., USA.

6. Millmore, S. (1977), The Measurement of the General Displacement Field Using Holographic Techniques, Master Thesis, The poly Technic Huddersfield, England.

7. Limtragool,J.(1982), Investigation of the Three-Dimensional Behavior of Cract-Tip Singularity by Holographic Interferometry, Ph.D. Dissertation, Carnegie-mellon University, USA.

8. Solecki, J.S. (1981), SHAPES-A: Finite Element Program for the Analysis of Elastic Three-Dimensional Cracks, Tech. Report SM-81-12, Dept. of Mech, Eng,. Carnegie-Mellon University, USA.

9. Hirth, J.P. and Lothe, J. (1968), Theory of Dislocations, McGraw-Hill Book Co., USA.